



## Intramuscular administration potentiates extended dwell time of mesenchymal stromal cells compared to other routes

LORENA R. BRAID<sup>1</sup>, CATHERINE A. WOOD<sup>1</sup>, DANIELLE M. WIESE<sup>1</sup> & BARRY N. FORD<sup>2</sup>

<sup>1</sup>Aurora BioSolutions Inc., Medicine Hat, Alberta, Canada, and <sup>2</sup>DRDC Suffield Research Centre, Casualty Management Section, Medicine Hat, Alberta, Canada

### Abstract

**Background.** Mesenchymal stromal cells (MSCs) offer great potential for diverse clinical applications. However, conventional systemic infusion of MSCs limits their therapeutic benefit, since intravenously (IV) infused cells become entrapped in the lungs where their dwell time is short. **Methods.** To explore possible alternatives to IV infusion, we used *in vivo* optical imaging to track the bio-distribution and survival of 1 million bioluminescent MSCs administered IV, intraperitoneally (IP), subcutaneously (SC) and intramuscularly (IM) in healthy athymic mice. **Results.** IV-infused MSCs were undetectable within days of administration, whereas MSCs implanted IP or SC were only detected for 3 to 4 weeks. In contrast, MSCs sourced from human umbilical cord matrix or bone marrow survived more than 5 months *in situ* when administered IM. Long-term survival was optimally achieved using low passage cells delivered IM. However, MSCs could undergo approximately 30 doublings before their dwell time was compromised. Cryo-preserved MSCs administered IM promptly after thaw were predominantly cleared after 3 days, whereas equivalent cells cultured overnight prior to implantation survived more than 3 months. **Discussion.** The IM route supports prolonged cell survival of both neo-natal and adult-derived MSCs, although short-term MSC survival was comparable between all tested routes up to day 3. IM implantation presents a useful alternative to achieve clinical benefits from prolonged MSC dwell time at a homeostatic implant site and is a minimally invasive delivery route suitable for many applications. However, optimized thaw protocols that restore full biological potential of cryo-preserved MSC therapies prior to implantation must be developed.

**Key Words:** bone marrow, cell survival, mesenchymal stromal cell, optical imaging, transplantation, umbilical cord

### Introduction

Mesenchymal stromal cells (MSCs) are a heterogeneous population of progenitor cells [1–5] exhibiting numerous therapeutically useful properties. Moreover, a growing body of evidence supports the notion that MSCs are highly suitable vectors for a range of therapeutic molecules, including growth factors, drugs and monoclonal antibodies [6–17]. Human umbilical cord perivascular cells (HUCPVCs) are a rich, well-characterized source of MSCs [18] highly amenable to engineering [6,7], stockpiling [19,20] and allogeneic transplantation [19,21,22]. HUCPVCs have exhibited robust clinical potential for a range of indications including inflammation [23–25], wound healing [24,26], myocardial infarction [25,27] and lung transplantation [28] and as gene therapy vectors for osteogenic repair [6] and bioweapons defense [7].

The consistent safety of administered MSCs [29–34] has been reported from numerous clinical trials. However, MSC therapies have had variable

success in meeting required endpoints in phase 2 and phase 3 clinical trials [35], in part due to limited persistence of cell transplants. The current standard practice for delivering cell therapies is by intravenous (IV) infusion. However, numerous studies have consistently demonstrated that IV-infused cells largely become trapped in the capillaries of the lungs, where they fail to survive longer than a few days [34,36–40]. This phenomenon truncates the potential therapeutic benefit of applied MSCs, a limitation cited in both clinical trials and animal studies [32,41,42].

There have been recent experimental demonstrations of MSCs as an active secretion platform to modulate the pharmacokinetics of therapeutic factors, including increasing numbers of reports that natural and engineered MSCs can provide sustained, continuous delivery of innate biomolecules and exogenous drugs and antibodies [8–17,43–45]. The reported correlations between cell persistence and systemic circulation of MSC-derived factors [7,36] suggest that non-conventional protocols may be useful to achieve

optimal sustained benefit from MSC therapies. Few studies, however, have combined cell bio-distribution data with serum profiles of MSC-secreted factors. Cells administered IV exhibit an acutely truncated serum profile of secreted factors, lasting less than 3 days [36]. In contrast, we recently reported that engineered MSCs, administered intramuscularly (IM), were still detectable at the implant site more than 100 days after transplantation where they continued to secrete a functional antibody into circulation [7]. We selected the IM administration route over IV infusion because our concept of use is for administration outside the boundaries of the clinic, in the field and for mass casualty scenarios. Here we sought to identify the key aspects of the previous study that generated such an unexpected and useful result, postulating that the observed persistence may be a consequence of the administration route, the early passage of the cells used in that study or the increased survival potential of the neo-natal cord-derived MSCs compared with adult-sourced MSCs such as bone marrow (BM). We also sought to identify the organs preferentially populated by MSCs administered by different routes, to aid in developing organ- or target-specific therapies for various indications.

Direct comparative evidence for MSC survival and bio-distribution following implantation by various routes is currently lacking. The parameters of individual studies, including cell source, isolation and expansion conditions, implantation routes and delivery vehicles, immune-competency, disease or injury state and type of animal model, combined with various cell labeling and detection methods preclude reliable comparisons between existing data sets.

The aim of this study was to execute a controlled, side-by-side comparison of the effects of delivery route and passage number (i.e., time in culture prior to implantation) on survival and distribution of a clinically relevant population of cells—HUCPVCs. In the present work, we performed a longitudinal comparison of the dwell time and bio-distribution of HUCPVCs administered by four clinically relevant routes: IV, intraperitoneal (IP), subcutaneous (SC) and IM. Next, we examined the effects of *in vitro* expansion and cryo-preservation on the dwell time of IM implanted HUCPVCs. Finally, we tested whether IM implantation also potentiates extended dwell time of human BM-derived MSCs. Taken together, our data identify IM implantation as an optimal route to achieve prolonged post-transplantation survival of MSCs, a critical factor in achieving controlled, sustained therapeutic benefit of applied MSCs. Finally, these data reveal that HUCPVCs can be subject to considerable expansion *in vitro* and still retain their persistence after IM implantation, and confirm a recent report that MSCs administered directly from cryogenic storage may be functionally compromised [46].

## Materials and methods

### Cell culture

HUCPVCs [22] cryo-preserved at passage 2 were provided by Tissue Regeneration Therapeutics (TRT), Inc. HUCPVCs were thawed according to TRT's proprietary standard operating procedures and expanded in Mesenchymal Stem Cell Growth Media—Chemically Defined (MSCGM-CD; Lonza). Passage 1 human BM-MSCs were also provided by TRT. BM-MSCs were recovered in isolation media—Alpha-Minimum Essential Medium (MEM; Life Technologies) supplemented with 15% MSC-Fetal Bovine Serum (FBS; Life Technologies)—then weaned to MSCGM-CD to facilitate direct comparison with HUCPVCs. At 70–80% confluence, MSCs were enzymatically detached from the culture vessel by brief incubation with TrypLE Select (Life Technologies), and re-seeded at a density of 4000 cells/cm<sup>2</sup>. Culture conditions were maintained at 37°C, 5% CO<sub>2</sub>, 80% relative humidity, with media replacement every 3–4 days.

For cryo-preservation, cells were enzymatically detached using TrypLE Select, pelleted by centrifugation at 149g, then resuspended in 50% MSCGM-CD and 50% EZ-CPZ (InCell) cryo-preservation media. Cryogenic vials were rapidly transferred to a CoolCell (Biocision) controlled-rate freezer and stored at -80°C overnight, then transferred to liquid nitrogen for cryogenic storage.

### Bioluminescent MSCs

For transient engineering of MSCs with the *firefly luciferase (ffluc)* gene, HUCPVCs and BM-MSCs at approximately 70% confluence in T150 flasks were incubated with a recombinant adenovirus serotype 5 encoding *ffluc* (Vector BioLabs), at 200 multiplicity of infection (MOI), suspended in 7.5 mL of MSCGM-CD (Lonza) without antibiotics for 3 h. Transduction media was removed and replaced with MSCGM-CD supplemented with antibiotic-antimycotic (Life Technologies) without washing. Twenty-four hours after transduction, cells were enzymatically detached using TrypLE Select, counted using a Millipore Scepter 2.0 (EMD Millipore), washed once in excess Hank's Balanced Salt Solution (HBSS; Life Technologies), then resuspended in an appropriate volume of HBSS to generate doses of 1 million cells per 75 µL. Cell viability in the dose cell suspension was verified by Trypan blue exclusion using a TC20 cell counter (BioRad) prior to implantation and again after administration of the final dose. Athymic mice received a single injection of 1 million cells in HBSS by IV infusion or IP, SC or IM injection.

To engineer MSCs with an integrated bioluminescent reporter gene, 2 million P2 HUCPVCs at

approximately 70% confluence in a T75 flask were incubated overnight with Cignal Lenti-luciferase (Qiagen) at 1 MOI, suspended in 6.0 mL MSCGM-CD without antibiotics. Lenti-transformants were selected by resistance to 500 ng/mL Puromycin (Life Technologies). Transformants were expanded for two passages, then cryo-preserved in EZ-CPZ (InCell) as described previously.

#### *Proliferation and differentiation assays*

Cell proliferation was assayed using the colorimetric Cell Counting Kit-8 (CCK-8; Sigma-Aldrich) assay. Native and engineered cells were seeded in a 96-well plate at a density of 1000 cells/well in 200  $\mu$ L of MSCGM-CD, with four replicate wells for evaluation at each of eight time points. Absorbance was measured at 450 nm every 24 h for 7 days using a Synergy HT (BioTek) microplate reader. Absorbance was normalized against the Day 1 measurement to account for variability in seeding density.

Multi-differentiation potential of MSCs was assayed by directed differentiation using commercially available adipogenic, osteogenic and chondrogenic media formulations. At least three replicate wells were assayed at each time point. Uninduced native and engineered cells were included as controls. No spontaneous induction was observed in uninduced cultures, except in adipogenesis assays where controls are incubated in maintenance medium containing a subset of the adipogenic factors, as specified by the assay manufacturer (Lonza).

Adipogenic human MSC (hMSC) differentiation Bulletkits (PT-3004, Lonza) were used to stimulate adipogenesis of native and engineered HUCPVCs. The lipophilic AdipoRed Assay Reagent (PT-7009) was used to quantify adipogenesis on days 7, 12, 18 and 25 after seeding. Relative fluorescent units (RFU) at 572 nm were quantified using a Synergy HT (BioTek) microplate reader. Cultures were subsequently imaged using fluorescence microscopy at 260X magnification on an EVOS digital microscope (Thermo Fisher Scientific).

Osteogenic potential was tested by directed differentiation using hMSC osteogenic differentiation Bulletkits (PT-3002, Lonza) according to the manufacturer's instructions. Mineralization was assessed on days 17 and 21 after induction using the OsteoImage Bone Mineralization Assay (PA-1503, Lonza). Hydroxyapatite was measured using fluorescence quantification at 488 nm using a Synergy HT (BioTek) microplate reader, followed by imaging at 260X magnification on an EVOS digital microscope (Thermo Fisher Scientific).

Chondrogenesis was induced in micromass pellet cultures incubated in chondrogenic MSC differentiation

Bulletkit media (PT-3003, Lonza) for 14 and 28 days, as per the manufacturer's instructions. Pellets were washed with Dulbecco's phosphate-buffered saline (DPBS; Life Technologies) and fixed with 10% neutral buffered formalin (Sigma-Aldrich). After fixing, the pellets were processed and embedded in paraffin using a TP1020 tissue processor (Leica). Microtome sections (4  $\mu$ m) were mounted on slides and subject to deparaffinization and antigen retrieval using citrate buffer pH 6.0 (Abcam) at 95°C for 15 min, followed by 20 min cooling and rehydration in PBS. Sections were blocked and permeabilized using PBS supplemented with 0.2% Triton X-100 (Sigma-Aldrich), 10% goat serum (Abcam) and 1% bovine serum albumin (BSA; Sigma-Aldrich) for 1 h at room temperature, followed by overnight incubation with 1° antibody (Rabbit anti-Collagen II; Abcam [ab34712]) diluted 1:50 in PBS with 0.1% Tween-20 (Sigma-Aldrich) plus 10% goat serum at 4°C. After washing with PBS, slides were incubated with Alexa488-conjugated anti-rabbit (Abcam) diluted 1:200 in PBS with 0.25% Triton X-100 plus 1% BSA for 90 min at room temperature. Sections were then mounted in Prolong Diamond Antifade Mountant (Molecular Probes, Life Technologies). Confocal images were captured at 400X magnification using a Quorum WaveFX laser scanning confocal microscope (Quorum Technologies Inc.) equipped with a Hamamatsu electron magnifying charge coupled device camera. Images were processed using Adobe Photoshop CS4.

#### *Animal studies*

Animal work was performed according to Canadian Council on Animal Care approved protocols and institutional standards of care. Eight- to ten-week-old athymic female BALB/c<sup>nu/nu</sup> mice (Charles River) were housed in pathogen-free conditions, and provided with sterilized water and irradiated chow *ad libitum*. Groups of three to five age-matched mice received an injection of 1.0 million HUCPVCs or BM-MSCs by the specified route. MSCs were administered IP, SC or IM as a single 75  $\mu$ L injection, or IV as a single 75  $\mu$ L injection in a tail vein. Control mice received an equivalent injection of HBSS delivery vehicle.

This study was predicated on prior observations and preliminary experiments, resulting in highly defined test parameters from the outset. To reduce the requirement for animals, experiments to examine passage number and MSC source on survival after IM implantation were performed simultaneously. Thus, data from a given group may have been used in more than one comparison; groups used in more than one comparison are stated in the relevant figure legend. In addition, representative animals were humanely killed at select time-points for *ex vivo* validation of the internal

source of bioluminescent regions of interest (ROIs) produced by *in vivo* optical imaging. Only the minimum number of animals required for confident interpretation of *in vivo* images was humanely killed.

### Optical imaging

Bioluminescence (BL) imaging was performed using the Xenogen In Vivo Imaging System (IVIS) Spectrum (PerkinElmer), equipped with Living Image 4.3.1. Eight minutes prior to imaging, mice received an IP injection of 150 mg/kg (150  $\mu$ L) D-luciferin Ultra salt solution (PerkinElmer). Mice were immobilized by isoflurane anesthesia delivered through a nose cone in the imaging chamber. Images were obtained within 1 h after cell transplantation (T0), and then periodically starting at 24 h post-injection and up to 154 days post-cell injection. For quantification, scale intensity of the longitudinal images was normalized and a ROI selected based on the signal intensity. The ROI was kept constant across comparison, and the total flux (photons emitted per second) measured.

BL from control groups (not shown) was minimal and used at each time-point to establish the background threshold. Control mice were injected with the HBSS delivery vehicle only and were used to establish the threshold for positive ROIs, particularly in maximal scans for weak signals. Controls were imaged in parallel with experimental mice, and received an IP injection of D-luciferin substrate 10 min prior to imaging. Faint liver-localized BL was consistently documented in maximal scans of control mice. *Ex vivo* imaging of experimental mice exhibiting liver-localized BL of similar intensity in maximal scans did not reveal *bona fide* ROIs, indicating that such BL was nonspecific background. Liver-localized ROIs were only validated *ex vivo* in IP-treated groups that exhibited ROIs with measurable BL above the threshold of negative controls. As such, signal intensities at or below this threshold were excluded from our analyses. A similar strategy was used for establishing signal-to-noise ratios for all other ROIs documented in the study.

For *ex vivo* validation, mice were humanely killed and tissues and organs rapidly harvested. Samples were rinsed with PBS, placed in a black dish and covered in ice-cold PBS containing 10 mmol/L adenosine triphosphate (ATP) and 30  $\mu$ g/mL D-luciferin substrate. All samples from a given mouse were imaged in a single frame.

For immunohistochemical analyses, dissected tissues and organs were washed with DPBS, placed in tissue cassettes and fixed by submersion in 10% neutral buffered formalin (Sigma-Aldrich). Tissues were subsequently embedded in paraffin using a Leica TP1020 tissue processor (Leica). Microtome sections (4–7  $\mu$ mol/L) were mounted on slides and subject

to deparaffinization and antigen retrieval using citrate buffer pH 6.0 at 95°C for 15 min, followed by 20 min of cooling and rehydration in PBS. Sections were blocked and permeabilized using PBS supplemented with 0.2% Triton X-100 (PBST; Sigma-Aldrich) and 5% goat serum (Abcam) for 2 h at room temperature, followed by overnight incubation with 1° antibodies in PBST with 5% goat serum at 4°C. After washing with PBS supplemented with 0.025% Triton X-100, sections were incubated with fluorescent conjugated 2° antibodies in PBST, washed three times in PBS and then mounted in SlowFade Mountant containing 4',6-diamidino-2-phenylindole (DAPI; Molecular Probes, Life Technologies). All antibodies were sourced from Abcam. Primary antibodies included Alexa 488 or Alexa 647 conjugated mouse anti-human nucleolin (364-5), rabbit anti-firefly luciferase (ab21176, ab185925) and goat anti-firefly luciferase (ab181640). Secondary antibodies used were Alexa Fluor 488 goat anti-rabbit (A-11008), Alexa Fluor 647 goat anti-rabbit (A-21245) and Alexa Fluor 488 donkey anti-goat (A-11055) highly cross-adsorbed immunoglobulins (Thermo Fisher). Confocal images were captured at 400X magnification using a Quorum WaveFX laser scanning confocal microscope (Quorum Technologies Inc.) equipped with a Hamamatsu electron magnifying charge coupled device camera. Images were processed using Adobe Photoshop CS4.

### Statistical analysis

In this study, *t* test comparisons, analysis of variance (ANOVA) with post hoc uncorrected Fisher Least Significant Difference (LSD) tests and nonlinear regression were performed using GraphPad Prism (Version 6.01, GraphPad Software). *In vivo* data represent the average BL obtained over three independent experiments, as specified in the figure legend. Error bars represent the standard deviation of averages shown in all figures.

## Results

### IM implantation potentiates HUCPVC survival

To facilitate longitudinal cell tracking *in vivo*, MSCs were engineered with the *ffluc* reporter gene using either an integrated or episomal expressible construct. Although the integrated marker permanently labels all cells and their progeny, reporter expression is insufficient for *in vivo* detection except at higher cell concentrations.

BL is significantly higher in cells transiently engineered with an episomal transgene, which better facilitates long-term tracking and minimizes the likelihood of confounding effects due to insertional mutagenesis. However, the episomal reporter is

stochastically diluted during cell division and precludes reliable evaluation of cell expansion in longitudinal studies. To compensate for these limitations, both types of engineered reporter cells were used in the study, to generate a more comprehensive data set for collective interpretation.

Two independent HUCPVC populations were established to stably express *ffluc* by lentiviral transduction (LLuc). These cell populations were used to detect post-transplantation cell proliferation or colonization, as would be evident from increasing or re-emerging BL. To facilitate long-term *in vivo* imaging, three donor populations of HUCPVCs were transiently engineered with *ffluc* by recombinant adenovirus transduction (pAdLuc). Due to multiple transgene copies per cell, the pAdLuc HUCPVCs produced BL 1 to 2 orders of magnitude higher than LLuc cells, and thus could be detected *in vivo* at much lower cell densities.

Standard proliferation and multi-differentiation assays were used to verify that engineering with *ffluc* does not alter the relevant biological characteristics of HUCPVCs. Bioluminescent HUCPVCs were assayed in direct comparison with native (unengineered) cells of the same cell population and passage number. Native controls exhibited nearly identical growth curves ( $r = 0.9961$ ;  $P < 0.0001$ ; Figure 1A), despite being derived from different donors. Bioluminescent engineering using either construct mildly attenuated proliferation. Growth kinetics of stably engineered HUCPVCs differed from unengineered controls by day 4 after seeding ( $P < 0.05$ ; Figure 1A), whereas deceleration of transiently engineered cells was not significant until day 6 ( $P < 0.05$ ; Figure 1A). These documented changes had minimal effect on the execution of the study because bioluminescent cell doses were readily obtained for the study within a day of native controls, even after cryo-preservation and revival of LLuc lines (not shown).

Conversely, bioluminescent HUCPVCs were slightly more responsive to directed differentiation than their native equivalents. LLuc (Figure 1B) and pAdLuc (Figure 1C) engineered HUCPVCs robustly responded to adipogenic, osteogenic or chondrogenic culture conditions as shown using fluorescence quantification and imaging of lipid droplets, hydroxyapatite mineralization and type II collagen, respectively. Decelerated proliferation concomitant with enhanced differentiation potential has been previously reported for engineered MSCs [7,47], and may indicate a mild stress response to the viral engineering process or to constitutive overexpression of the transgene.

We first tested the impact of administration route on bio-distribution and cell survival using *in vivo* optical imaging of 1 million bioluminescent HUCPVCs administered by four clinically relevant routes—IV,

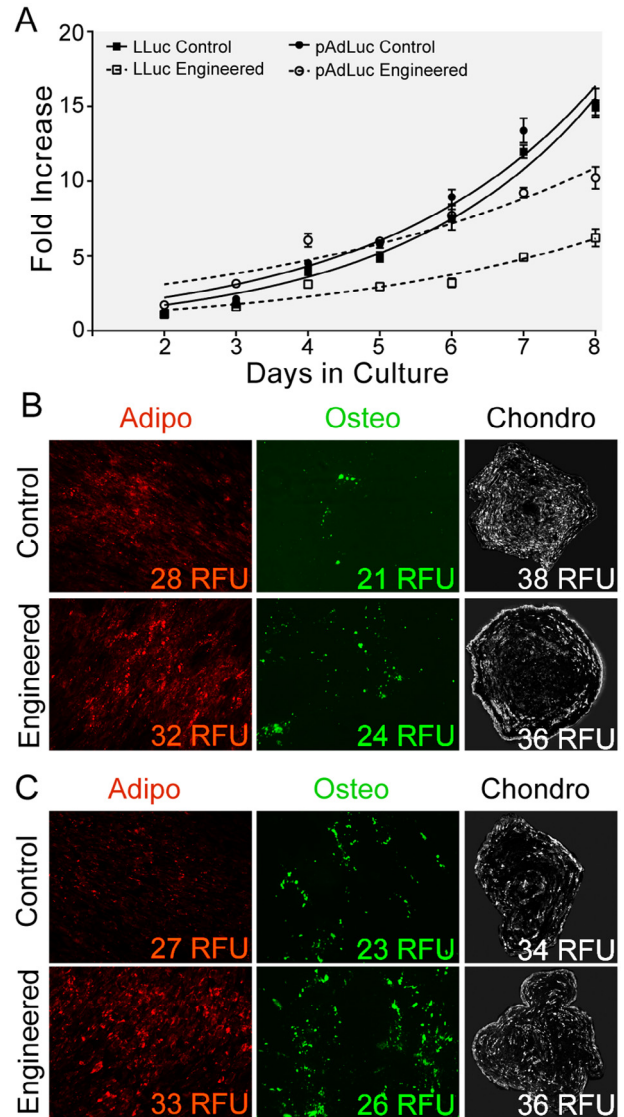


Figure 1. Characterization of bioluminescent HUCPVCs. The proliferation and multi-lineage differentiation potential of *ffluc*-expressing HUCPVC lots, engineered via LLuc or pAdLuc transduction, were compared with equivalent unengineered (Control) cells. (A) Proliferation was assayed daily as a function of metabolic activity using CCK-8 and normalized against measured activity on Day 1. Exponential cell growth was fitted using a non-linear regression curve. Control lots exhibited nearly identical growth curves ( $r = 0.9961$ ;  $P < 0.0001$ ). Doubling time of LLuc engineered cells decelerated by day 4, but did not stall. Decelerated proliferation of pAdLuc engineered cells was not apparent until day 6. (B–C) In multi-lineage differentiation assays, (B) LLuc and (C) pAdLuc engineered HUCPVCs are robustly induced into adipocytes (AdipoRed), osteocytes (OsteoImage) and chondrocytes (type II Collagen), similar to unengineered (Control) equivalents. RFU are shown for each sample. Error bars represent SD;  $n = 4$  for proliferation assays,  $n = 3$  for differentiation assays. Abbreviation: SD, standard deviation.

IP, SC and IM. For this study, LLuc-engineered HUCPVCs were used to evaluate short-term cell dynamics after transplantation, and to detect cell expansion post-transplantation. Luminescence captured

on the surface of an intact animal may not accurately reflect the position of the internal light source because emitted photons are absorbed by hemoglobin. To validate the signal source of documented ROIs, representative animals were humanely killed at select time points and their dissected organs re-imaged *ex vivo*.

One hour after IV infusion, intense BL was detected in bilateral ROIs in the thoracic cavity (Figure 2A). These ROIs correlated with the lungs, as demonstrated using three-dimensional image reconstruction (not shown) and *ex vivo* imaging of isolated lungs (Figure 2A and Supplemental Figure S1). BL in the lungs had substantially decreased after 24 h and was not detected above background after 7 days (Figure 2A). Our findings are consistent with numerous reports that IV-infused MSCs become lodged in the lungs and fail to persist there for more than several days [36–39]. We also noted that considerable BL was retained at the tail vein injection site, even after BL was lost from the lungs (not shown). This phenomenon has been reported previously [48] and is adventitious evidence for extravascular survival of implanted MSCs.

Bioluminescent HUCPVCs administered IP exhibited dynamic and somewhat stochastic distribution immediately following implantation (Figure 2B), and overall failed to persist at any fixed location. In the first 3 days following implantation, BL was most frequently detected in the liver and spleen and associated with the gastrosplenic ligament (Figure 2B), although spatial and temporal intensity varied between animals. When BL was no longer detectable in these organs and tissues, it could be detected in the kidneys (Figure 2B) just prior to complete loss of the signal. BL was not detected in any other organs (Supplemental Figure S1). At most, BL was detected in the liver region for up to 21 days post-transplantation in 20% of recipient mice (Figure 2B).

By contrast, bioluminescent HUCPVCs administered SC at the nape of the neck remained *in situ* in healthy animals (Figures 2C and 2D). Statistically significant BL was never detected at distal sites. Only 60% of mice were faintly positive for BL at day 14 and 21, and no BL was detected at day 30 or later (Figures 2C and 2E).

Strikingly, BL from HUCPVCs implanted in the left hind limb was still detected at the site of IM injection 104 days after implantation in 100% of recipient mice (Figure 2D and 2E). BL was not detected at remote sites in healthy animals at any time during the study (Supplemental Figure S1 and Supplemental Figure S2), although cutaneous BL was detected in a single mouse that sustained a cage wound late in the study (not shown). Interestingly, *ex vivo* imaging of the left hind limb within 7 days of implantation

revealed two distinct ROIs—one corresponding to the syringe entry site, the other to the site of cell deposition (Figure 2D). At the end of the study, BL was only documented at the syringe entry site (Figure 2D), suggesting that MSCs may have actively aggregated at the wound site in response to local inflammatory signals.

Quantification of luminescence revealed two additional trends. First, total BL was highly similar between the IP-, SC- and IM-treated groups in the first 3 days following implantation, followed by a precipitous decrease in BL by day 7 (Figure 2E). The IV infused group displayed a similar trend, although overall BL was significantly lower due to depth of the signal; the first significant decrease in BL in this group occurred at day 3 rather than day 7, and no signal was detected *in vivo* after day 7. This suggests that similar short-term cell survival can be achieved by any of these administration routes. Second, no instance of increased or re-emerging BL was ever observed in the study, suggesting that the implanted HUCPVCs do not proliferate at a significant rate after implantation in healthy animals, nor do they exhibit a propensity for colonization.

#### *HUCPVCs cultured to passage 6 retain their potential for extended survival*

Having demonstrated that the IM route potentiates extended dwell time of HUCPVCs, we next examined the effect of passage, or *in vitro* expansion, on the survival of IM implanted HUCPVCs. For this analysis, transiently transduced pAdLuc HUCPVCs were used to generate significantly higher BL signals and thereby increase the threshold and sensitivity of optical imaging. Cells at passage 3, 6, 7 or 11 were engineered with the *ffluc* reporter and implanted IM in the left thigh muscle. Cell populations typically doubled 4 to 5 times per passage. BL was detected at equivalent levels in 100% of mice treated with passage 3 or passage 6 HUCPVCs at days 30 and 61 ( $P > 0.05$ ), although BL was slightly higher in passage 6 HUCPVCs at day 104 (Figure 3A). The first of the three independent experiments was carried out to day 154, and both groups remained positive for BL at this time point (not shown). However, 20% of mice treated with passage 7 cells lost BL by day 14 (Figure 3B); the remaining mice exhibited BL equivalent to passage 3 and passage 6 groups until day 104. Dwell time of passage 11 HUCPVCs was significantly reduced compared with the earlier passage cells. By day 14, BL was undetectable in 60% of mice from this group, and only 20% of passage 11-treated mice were positive for the BL at the end of the study (Figure 3B). Moreover, BL from passage 11–implanted cells was first significantly reduced compared with the other groups by day 7 ( $P < 0.05$ ; Figure 3A), revealing that short-term

persistence was also attenuated. In addition, BL in mice treated with passage 6 or passage 7 cells decreased more between days 3 and 7 than passage 3 cells (Figure 3A). However, by day 30, BL was equivalent

in passage 3-, passage 6- and passage 7-treated groups ( $P > 0.5$ ) and was maintained to day 104 (Figure 3A).

To verify the presence of MSCs after such an extended time, we probed paraffin-embedded muscle

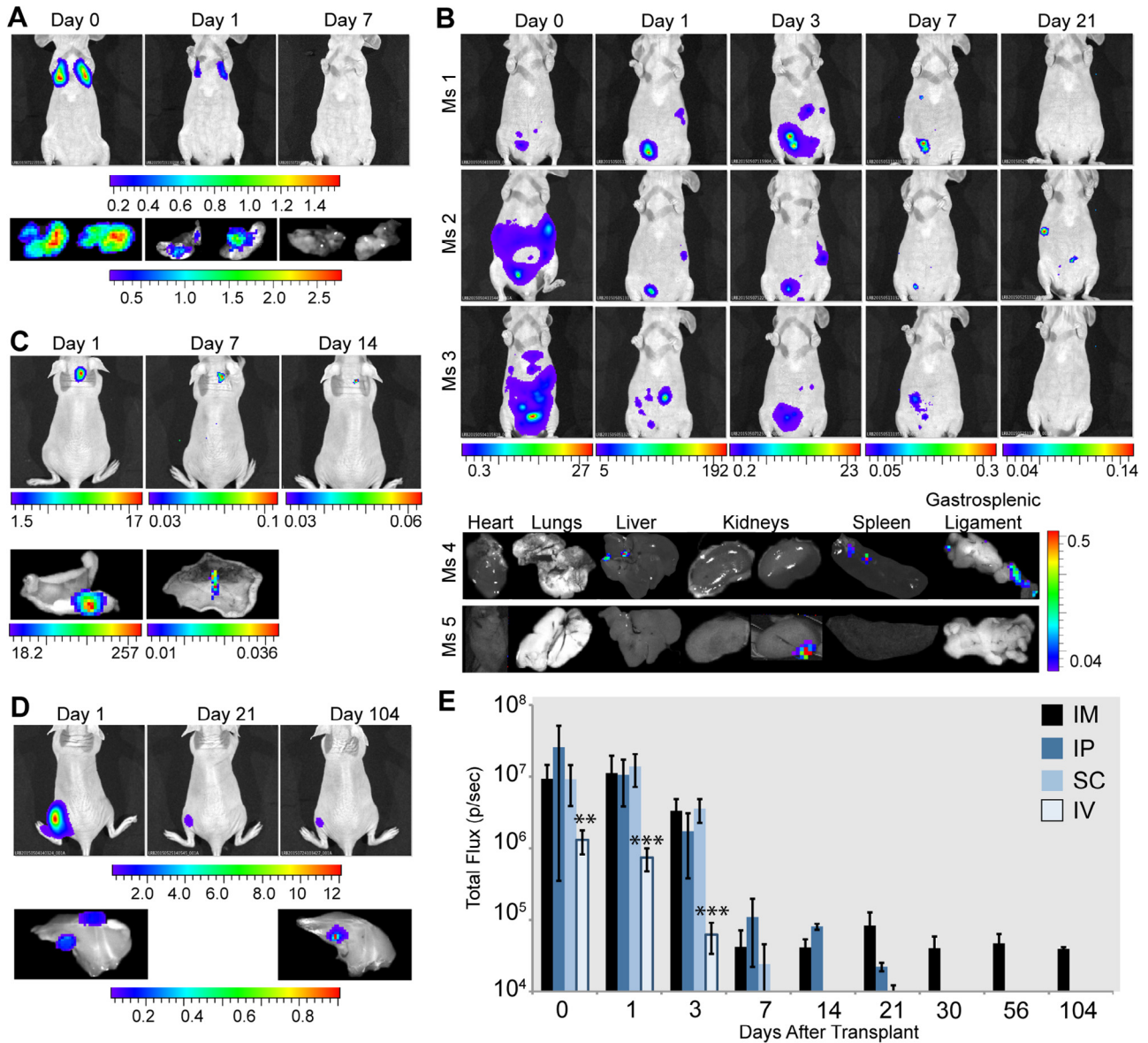


Figure 2. Administration route affects bio-distribution and dwell time of LLuc HUCPVCs. Longitudinal *in vivo* images of representative mice are shown at select time-points. Organs imaged *ex vivo* are from other representative mice terminated at the specified times to validate signal source. BL is represented by pseudocolored heat maps where values in scale bars are  $\times 10^5$  photons/sec/cm<sup>2</sup>/sr. (A) BL from IV infused HUCPVCs localized to the lungs within hours after transplantation (day 0). Within 24 h, BL was considerably reduced. By day 7, no BL remained in the lungs. (B) BL from IP administered HUCPVCs was temporally and spatially dynamic. Within the first 3 days, BL was consistently detected in the liver and spleen and was associated with the gastrosplenic ligament, although at varying relative intensities (Ms 4). BL was typically lost from these organs and connective tissue between days 3 and 21 (Ms 1–3) and concomitantly localized to the kidneys (Ms 5) before decreasing below the detectable threshold. (C) HUCPVCs administered SC remained *in situ*. BL rapidly diminished between days 3 and 7, and decreased to threshold limits by day 14. (D) HUCPVCs administered IM also remained *in situ* but remained detectable to the end of the study, day 104. (E) BL was quantified from all *in vivo* ROIs at each time-point as Total Flux (photons per second). Administration route had minimal effect on dwell time for the first 3 days after transplantation, and all groups exhibited a considerable loss of BL between days 3 and 7. IV infused cells were not detected after day 7, whereas SC implanted cells were not reliably detected after day 14. IP implanted cells were detectable to day 21 in 30% of mice. By contrast, BL from IM implanted HUCPVCs stabilized after day 7 and was detected until the end of the study, day 104. BL did not increase or re-emerge during the study. The graph shows averages  $\pm$ SD from three independent experiments,  $n = 3$ –5 mice per group per experiment. ( $*P < 0.05$ ,  $**P < 0.005$  and  $***P < 0.0005$  using Student *t* test.) See also Supplemental Figures S1 and S2. Abbreviation: Ms, mouse.

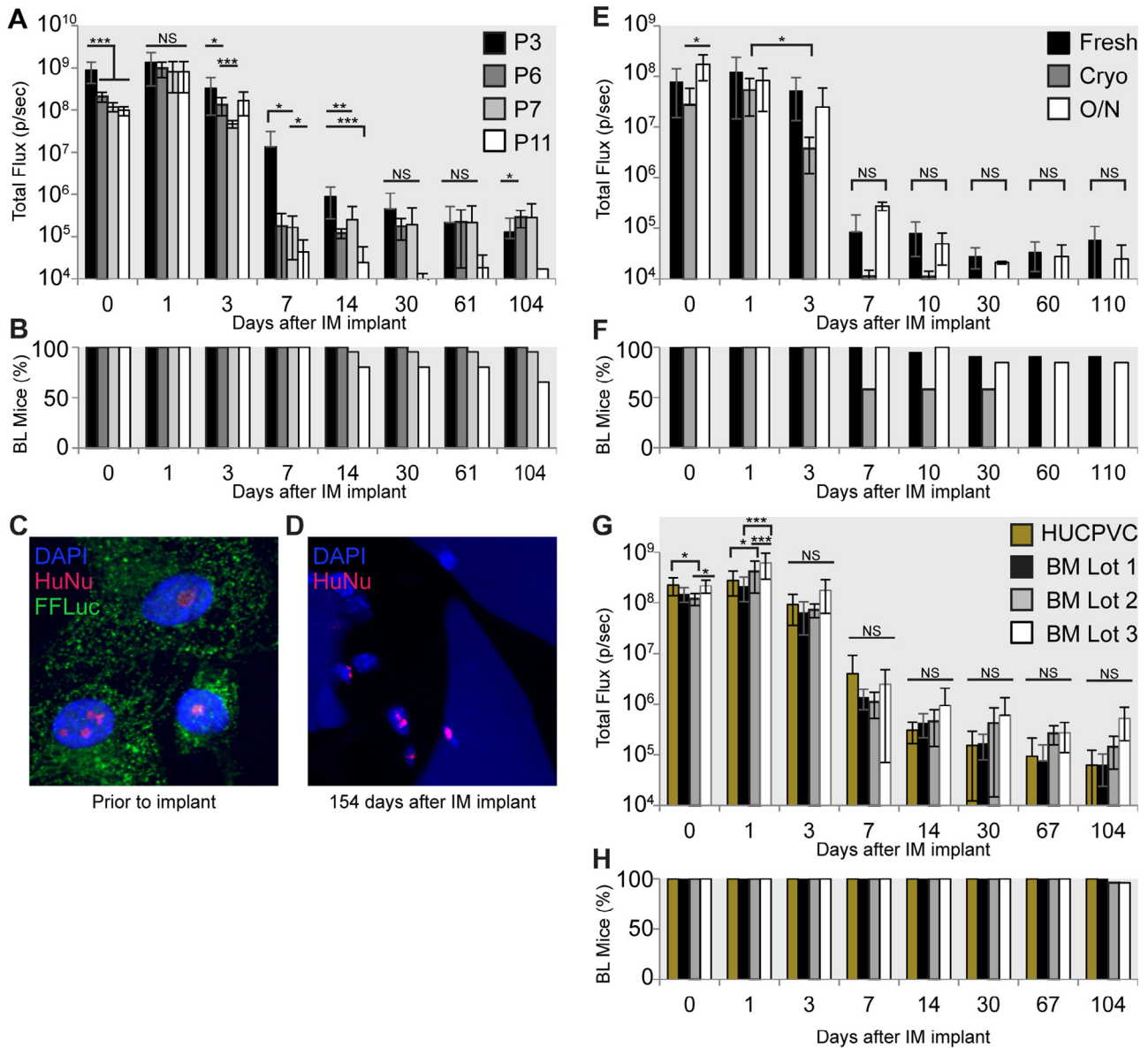


Figure 3. Evaluation of factors affecting dwell time of IM-implanted MSCs. Nude mice received an IM injection of 1 million pAdLuc HUCPVCs (A–F) or pAdLuc BM-MSCs (G, H) in the left hind limb. BL from the engineered cells was captured using *in vivo* optical imaging and quantified as total flux (A, E, G). Percentage of total mice positive for BL at each time-point is shown in B, F and H. (A, B) Extended *in vitro* expansion of HUCPVCs to P6 or P7 has minimal effect on cell persistence after IM implantation. P3 and P6 cells produce equivalent BL to day 104, whereas cells expanded to P7 show slightly diminished dwell time. P11 cells exhibit markedly reduced BL after day 3 (A) and truncated dwell time (B) in comparison with earlier passage cells. (C) The immunocytological staining patterns of HuNu (magenta) and FFLuc (green) in pAdLuc HUCPVCs were documented in cultured cells prior to implantation. FFLuc localizes to cytoplasmic peroxisomes, whereas HuNu specifically localizes to nucleosomes within DAPI-stained nuclei (blue). A single plane confocal image at 400x magnification is shown. (D) A representative photomicrograph of immunohistochemically stained sections of the left hind limb muscle harvested 154 days after IM implantation of pAdLuc HUCPVCs reveals DAPI-stained nuclei (blue) also positive for HuNu (magenta). FFLuc was not detectable in paraffin-embedded sections at any time-point. A 4  $\mu$ mol/L stack of confocal images captured at 400x magnification is shown. (E, F) The dwell time of HUCPVCs administered directly from cryo-preservation is significantly compromised. Overnight culture of these cells prior to implantation recovers their innate capacity for long-term survival at the IM implantation site. (G, H) One million P3 BM-MSCs from three different donors were engineered with pAd-FFLuc and implanted IM in the left hind limb. *In vivo* optical imaging revealed that BM-MSCs exhibit longitudinal BL consistent with HUCPVCs, suggesting that the IM route is more critical to long-term persistence than the MSC source. (A, E) Average BL from three independent experiments, five mice per group, is shown. Error bars represent SD. (\* $P < 0.05$ , \*\* $P < 0.005$  and \*\*\* $P < 0.0005$  using Student *t* test.) (G) Average BL from two technical replicates, three mice per BM-MSC group, is shown. P3 HUCPVCs are the same group shown in (A, B), as these studies were carried out in parallel. (\* $P < 0.05$ , \*\* $P < 0.005$  and \*\*\* $P < 0.0005$  using uncorrected Fisher LSD test.) Abbreviations: HuNu, human nucleolin; NS, no statistical significance; P, passage.

sections of these mice for human nucleolin (HuNu) and FFLuc antigens. We first validated the detection pattern of these antibodies on cultured *ffluc* HUCPVCs, captured using confocal microscopy (Figure 3C). Indeed, at 154 days post-implantation a small percentage of DAPI-stained nuclei were also positive for HuNu, confirming the presence of exogenous human cells (Figure 3D). These human nuclei were most commonly observed between muscle fibers, consistent with the report by Vilalta *et al.* using IM-implanted adipose-derived MSCs [49]. Taken together, HUCPVCs retain their potential for long-term persistence after IM implantation until passage 6 or passage 7, providing an opportunity for considerable *in vitro* cell expansion and stockpiling.

#### *Dwell time of freshly thawed HUCPVCs is compromised*

We also evaluated the dwell time of *ffluc*-engineered HUCPVCs implanted immediately post-thaw from cryo-storage, in direct comparison with equivalent cells 48 h after engineering (without cryo-preservation), and equivalent engineered cells thawed from cryo-storage and cultured overnight prior to implantation. Cryogenically stored *ffluc* HUCPVCs were thawed according to standard protocols, including centrifugation and resuspension in fresh media to remove cryogenic media. For direct implantation, viable cells were counted using Trypan blue exclusion to ensure implantation of 1 million viable cells, then centrifuged and resuspended in an appropriate dose volume. After all cell transplantations were performed, the remaining contingency volume was injected into a flask containing media and cultured; the cells adhered and proliferated normally, indicating that they had not been physically compromised by the thaw and injection procedure. Cells allowed to recover prior to implantation were similarly thawed, then transferred to culture flasks overnight. In all cases, viable cells were counted prior to centrifugation and resuspension in an appropriate dose volume, then immediately administered.

Cells administered directly after thawing exhibited markedly compromised dwell time; BL was only detectable up to day 3 in 85.7% of treated mice (Figure 3E;  $P < 0.05$ ). The remaining mice (14.3%) maintained a BL signal between days 7 and 30 (Figure 3F), but luminescence was barely detectable above threshold (Figure 3E). Culturing these cryo-preserved cells overnight prior to implantation vastly improved their post-transplantation survival. Mice treated with pAdLuc HUCPVCs of the same population and passage number, fresh from culture or recovered overnight after cryo-preservation, exhibited similar longitudinal BL intensities and dwell time ( $P > 0.05$  at days 0–10; Figure 3E). These data indicate that the persistence of engineered HUCPVCs

is uncompromised by cryo-preservation if the cells have an opportunity to more fully recover prior to transplantation.

#### *IM implantation also potentiates survival of human BM-MSCs*

Finally, we tested whether IM implantation could potentiate long-term survival of another clinically relevant MSC population. Three donor populations of human BM-MSCs were cultured and transiently engineered with the *ffluc* gene using conditions identical to pAdLuc HUCPVCs. One million BM-MSCs were implanted in the left thigh muscle of recipient nude mice. Consistent with our previous findings, BL from all three populations of BM-MSCs was detectable 110 days after IM implantation (Figure 3G). *Ex vivo* imaging validated the source of BL as the injection site in the hind limb (Supplemental Figure S2). Interestingly, both the longitudinal BL intensities (Figure 3G) and dwell time (Figure 3H) of BM-MSCs closely followed that of HUCPVCs. Taken together, the IM route of administration can potentiate extended dwell time of both neo-natal and adult MSCs, and offers an alternative to conventional IV infusion to achieve sustained benefit from MSC cell therapies.

## Discussion

The aim of this study was to characterize the dwell time and bio-distribution of clinically relevant MSC doses in a controlled setting. Previous studies using sensitive methods, such as quantitative polymerase chain reaction (qPCR), have detected minute quantities of DNA from implanted MSCs in a wide range of organs post-transplantation [2,41,50,51]. While we predict that the MSCs in our study may have similarly distributed at trace levels, our focus here was to establish the post-transplantation behavior of MSC quantities sufficient to generate therapeutically useful benefits.

While it is evident from this study that IM implantation potentiates dwell time far exceeding that of IV, IP or SC routes, it is notable that within 3 days of implantation, changes in total BL were comparable across transplant groups. This suggests that for acute cell therapy benefits, route of administration is dispensable for cell survival, and the delivery protocol should rather be prioritized based on limitations and requirements for a given indication. For sustained cell therapies, however, particularly those in which MSCs are exploited as delivery vectors for bio-molecules intended for systemic circulation, implantation route can have considerable impact on therapeutic success and should be considered during development of therapeutic protocols.

The notion of using IM implantation as an alternative to IV infusion has been explored for limb-specific indications in both pre-clinical [51–53] and clinical studies [54–59]. Most recently, BM-MSCs engineered with vascular endothelial growth factor (VEGF), administered IM in a mouse model of critical limb ischemia, were detected in the hamstring muscle up to 21 days post-transplantation using optical imaging, or up to 4.5 months using PCR [51]. These results are consistent with our report, although our homeostatic animal model makes an important distinction from the preferential survival of exogenous MSCs at a local inflamed site [48]. Whether the muscle provides a permissive microenvironment that better supports MSC survival than the other routes tested is unknown.

The biological characteristics of the long-lived MSCs at the IM implantation site are not yet known. Tools to definitively track, identify, characterize and recover human cells after transplantation in animal models have improved drastically in recent years, but are not yet adequate to fully answer many important, unresolved questions about the ultimate fate of MSCs after implantation. Antibodies raised against human nuclear antigens, like the one used in this study, are valuable means to identify human nuclei after transplantation. However, there are still no human-specific cytoplasmic or cell surface markers to identify associated cell bodies in the milieu of dense tissue sections and to definitively co-register any other immunolabels or to interpret morphological or phenotypic data.

There is, however, compelling data to suggest that the IM implanted cells remain metabolically active. First, the luciferase enzyme requires ATP and  $Mg^{2+}$ , in addition to luciferin substrate, to generate BL [60]. By genetically encoding luciferase as the visual reporter, rather than a fluorescent molecule, BL also reports on the metabolic activity of the host cell. Indeed, the ATP requirement for BL was so acute in our study that within minutes of euthanasia BL was lost as ATP was consumed by the cells, and tissues and organs had to be rapidly submerged in a solution of ATP and luciferin to recover BL for *ex vivo* imaging. Moreover, our previous data demonstrated active secretion of a recombinant antibody by IM implanted HUCPVCs for more than 100 days [7]. Taken together, detection of both the genetically encoded visual and secreted reporters for more than 100 days supports the notion that IM implanted MSCs remain metabolically active, at least for several months after implantation.

Despite substantial effort, using multiple combinations of published anti-FFLuc antibodies and protocols on tissue sections from animals 1 day after implantation and thus exhibiting robust BL, we were unable to detect luciferase using immunohistochemical staining of wax-embedded tissue sections. As such,

we were unable to perform co-labeling experiments to detect false-positive BL from macrophages, which may have acquired the transgene by scavenging dead MSCs. Although we cannot exclude the presence of false positives from our data set at this time, we do not believe that they contribute to the final conclusions of the study. The use of a genetically encoded reporter and the fact that equivalent data was obtained using both an integrated and episomal reporter construct minimize the likelihood that confounding BL was produced by passive transfer of the reporter transgene or by incomplete catabolism of the transgene after scavenging. The distinct BL profiles documented using MSCs from different passage numbers and fresh versus cryo-preserved cells that terminated months apart also provide evidence that a massive die-off, and consequent scavenging, of MSCs early in the study does not generate long-term BL.

A previous study using human adipose-derived MSCs also described extended cell survival following IM implantation compared with IV infusion [49]. However, these authors concluded that both IM and IV implanted cells preferentially colonized the liver [49]. Although we also observed low-intensity BL in the liver during maximal sensitivity scans for weak signals, it was classified as nonspecific background since equivalent BL was also documented in control mice that were not treated with MSCs. Further, we were unable to demonstrate that such BL represented true cell localization using *ex vivo* imaging. Consistent with our findings, however, Creane *et al.* recently reported that MSCs implanted IM in healthy mice were only retained at the muscle site and not at distal murine tissues, as determined using qPCR of human *alu* sequences [61]. In our study, MSCs were highly retained at both the IM and SC implantation sites, revealing that these two routes present opportunities for controlled MSC dosing, in contrast to dynamic cell distribution among visceral tissues and organs as a consequence of IP injection.

The reported inconsistencies between MSCs isolated using different extraction methods or from different tissues and MSCs propagated in different expansion media, particularly in the presence or absence of serum, are a significant hurdle in the development of MSC therapies. Our findings appear to transcend these inherent differences, at least for BM and cord-derived MSCs, and thus have broad clinical relevance. We first documented prolonged IM dwell time using HUCPVCs isolated and cultured in alpha-MEM supplemented with 15% animal serum [7]. In the current report, HUCPVCs were isolated using a revised protocol and cultured in serum-free media using protocols recapitulating those developed for good manufacturing practice (GMP)-compliant manufacturing by the cell provider, TRT Inc. Thus, IM

administration not only prolonged the survival of HUCPVCs isolated and cultured by different methods, but also extended the dwell time of distinct BM- MSC populations isolated using a third technique.

MSCs are a heterogeneous population of cells [2–5,22]. The data presented here suggest that the MSC milieu may include a subpopulation with higher potential for long-term survival than other cells in the population, particularly when administered IM. Intense BL was comparable for the first 3 days after IM implantation, followed by marked decrease by day 7. This trend was consistent between all administration routes tested. Fourteen days after IM implantation, however, BL stabilized and was generally maintained until the end of the study. In animals treated with higher passage cells, however, BL after day 14 was specifically compromised, whereas BL in the first 3 days was similar to lower passage cells.

Therefore, we propose that a subpopulation of MSCs with strong survival potential exists at a high ratio immediately after isolation, but is gradually lost during *in vitro* expansion. Indeed, cell cycle kinetics appear to have an important role in the engraftment and migratory potential of stem cells [2,62–65]. Thus, it is plausible to envision a subpopulation of asynchronous MSCs with high engraftment potential that are selected against during prolonged cell expansion. We are currently analyzing the gene expression profile of HUCPVCs during *in vitro* expansion from isolation to natural senescence, with the aim of identifying novel markers of this waning subpopulation of potent engrafters. This data will inform on the appropriate expansion time to obtain the maximum number of long-term surviving HUCPVCs for clinical applications. However, whether such a population also possesses potent immune-modulatory and/or tropic responsiveness to inflammation or whether these properties are inherent to shorter-lived cells remain to be elucidated.

We documented that the most direct route of cell recovery—simply thawing from cryo-storage, washing and administering IM—compromised the long-term persistence of HUCPVCs, while allowing the cells to recover overnight prior to implantation reversed this effect. Previous reports have suggested that the therapeutic potential and viability of cryogenically stored MSCs can be attenuated and that variations in both the cryo-storage and thawing procedures can affect these outcomes [46,66–68]. This accumulating evidence reveals a gap in bench-to-bedside translation of off-the-shelf cell therapies and must be resolved. There is not only a need for specific protocols that rapidly recover these innate biological characteristics of MSCs after thawing, but also for development of standardized assays to assure delivery of cell therapies with full potency after cryo-preservation.

## Conclusion

Taken together, we propose that the IM route presents a minimally invasive alternative to conventional IV infusion for applications beyond local limb injury. IM administration is particularly beneficial for MSC treatment modalities premised on secreted biomolecules. We have shown that IM implanted HUCPVCs continuously secrete an exogenous antibody that confers protection against a viral bioweapon for more than 3 months [7], whereas Mao *et al.* reported that IM administered umbilical cord MSCs improved cardiac function in a rat model of dilated cardiomyopathy [69]. These results support the notion that IM situated MSCs can provide sustained delocalized benefit for diverse applications. Moreover, IM is a field-deployable administration route. The data described herein brings the notion of developing novel cell therapeutics for uses beyond the clinic into the realm of possibility.

## Acknowledgments

The authors wish to thank Tissue Regeneration Therapeutics Inc., Toronto, Canada, for provision of cells, and Dr. J.E. Davies for critical review of the manuscript. Funding was provided by Public Service and Procurement Canada (PSPC) contracts W7702-145669 and W7702-155729 to Aurora BioSolutions Inc.

**Disclosure of interests:** L.R. Braid is an officer and shareholder of Aurora BioSolutions Inc. C.A. Wood and D.M. Wiese are employees of Aurora BioSolutions Inc.

## References

- [1] Sacchetti B, Funari A, Remoli C, Giannicola G, Kogler G, Liedtke S, et al. No identical “mesenchymal stem cells” at different times and sites: human committed progenitors of distinct origin and differentiation potential are incorporated as adventitial cells in microvessels. *Stem Cell Reports* 2016;6:897–913.
- [2] Lee RH, Hsu SC, Munoz J, Jung JS, Lee NR, Pochampally R, et al. A subset of human rapidly self-renewing marrow stromal cells preferentially engraft in mice. *Blood* 2006; 107:2153–61.
- [3] Dominici M, Le Blanc K, Mueller I, Slaper-Cortenbach I, Marini F, Krause D, et al. Minimal criteria for defining multipotent mesenchymal stromal cells. The International Society for Cellular Therapy position statement. *Cytotherapy* 2006;8:315–17.
- [4] Covas DT, Panepucci RA, Fontes AM, Silva WA Jr, Orellana MD, Freitas MC, et al. Multipotent mesenchymal stromal cells obtained from diverse human tissues share functional properties and gene-expression profile with CD146+ perivascular cells and fibroblasts. *Exp Hematol* 2008;36:642–54.
- [5] Sarugaser R, Hanoun L, Keating A, Stanford WL, Davies JE. Human mesenchymal stem cells self-renew and differentiate

- according to a deterministic hierarchy. *PLoS ONE* 2009; 4:e6498.
- [6] Vallejo CE. Characterization of Genetically Modified HUCPVCs as an Osteogenic Cell Source. Toronto, ON, Canada: University of Toronto; 2013.
  - [7] Braid LR, Hu WG, Davies JE, Nagata LP. Engineered mesenchymal cells improve passive immune protection against lethal Venezuelan equine encephalitis virus exposure. *Stem Cells Transl Med* 2016;5:1026–35.
  - [8] Hodgkinson CP, Gomez JA, Mirotsov M, Dzau VJ. Genetic engineering of mesenchymal stem cells and its application in human disease therapy. *Hum Gene Ther* 2010;21:1513–26.
  - [9] Kumar S, Chanda D, Ponnazhagan S. Therapeutic potential of genetically modified mesenchymal stem cells. *Gene Ther* 2008;15:711–15.
  - [10] Frank RT, Najbauer J, Aboody KS. Concise review: stem cells as an emerging platform for antibody therapy of cancer. *Stem Cells* 2010;28:2084–7.
  - [11] Compte M, Cuesta AM, Sánchez-Martín D, Alonso-Camino V, Vicario JL, Sanz L, et al. Tumor immunotherapy using gene-modified human mesenchymal stem cells loaded into synthetic extracellular matrix scaffolds. *Stem Cells* 2009;27:753–60.
  - [12] Balyasnikova IV, Ferguson SD, Sengupta S, Han Y, Lesniak MS. Mesenchymal stem cells modified with a single-chain antibody against EGFRvIII successfully inhibit the growth of human xenograft malignant glioma. *PLoS ONE* 2010;5:e9750.
  - [13] Balyasnikova IV, Franco-Gou R, Mathis JM, Lesniak MS. Genetic modification of mesenchymal stem cells to express a single-chain antibody against EGFRvIII on the cell surface. *J Tissue Eng Regen Med* 2010;4:247–58.
  - [14] Young JS, Kim JW, Ahmed AU, Lesniak MS. Therapeutic cell carriers: a potential road to cure glioma. *Expert Rev Neurother* 2014;14:651–60.
  - [15] Wyse RD, Dunbar GL, Rossignol J. Use of genetically modified mesenchymal stem cells to treat neurodegenerative diseases. *Int J Mol Sci* 2014;15:1719–45.
  - [16] Cucchiari M, Venkatesan JK, Ekici M, Schmitt G, Madry H. Human mesenchymal stem cells overexpressing therapeutic genes: from basic science to clinical applications for articular cartilage repair. *Biomed Mater Eng* 2012;22:197–208.
  - [17] Liu LN, Wang G, Hendricks K, Lee K, Bohnlein E, Junker U, et al. Comparison of drug and cell-based delivery: engineered adult mesenchymal stem cells expressing soluble tumor necrosis factor receptor II prevent arthritis in mouse and rat animal models. *Stem Cells Transl Med* 2013;2:362–75.
  - [18] Davies JE, Walker JT, Keating A. Concise review: Wharton's jelly: the rich, but enigmatic, source of mesenchymal stromal cells. *Stem Cells Transl Med* 2017;6:1620–30.
  - [19] Ennis J, Gotherstrom C, Le Blanc K, Davies JE. *In vitro* immunologic properties of human umbilical cord perivascular cells. *Cytotherapy* 2008;10:174–81.
  - [20] Schugar RC, Chirieleison SM, Wescoe KE, Schmidt BT, Askew Y, Nance JJ, et al. High harvest yield, high expansion, and phenotype stability of CD146 mesenchymal stromal cells from whole primitive human umbilical cord tissue. *J Biomed Biotechnol* 2009;2009:789526.
  - [21] Ennis J, Sarugaser R, Gomez A, Baksh D, Davies JE. Isolation, characterization, and differentiation of human umbilical cord perivascular cells (HUCPVCs). *Methods Cell Biol* 2008;86:121–36.
  - [22] Sarugaser R, Lickorish D, Baksh D, Hosseini MM, Davies JE. Human umbilical cord perivascular (HUCPV) cells: a source of mesenchymal progenitors. *Stem Cells* 2005;23:220–9.
  - [23] Gomez-Aristizabal A, Davies JE. The effects of human umbilical cord perivascular cells on rat hepatocyte structure and functional polarity. *Biochem Cell Biol* 2013;91:140–7.
  - [24] Shohara R, Yamamoto A, Takikawa S, Iwase A, Hibi H, Kikkawa F, et al. Mesenchymal stromal cells of human umbilical cord Wharton's jelly accelerate wound healing by paracrine mechanisms. *Cytotherapy* 2012;14:1171–81.
  - [25] Dayan V, Yannarelli G, Billia F, Filomeno P, Wang XH, Davies JE, et al. Mesenchymal stromal cells mediate a switch to alternatively activated monocytes/macrophages after acute myocardial infarction. *Basic Res Cardiol* 2011;106:1299–310.
  - [26] Zebardast N, Lickorish D, Davies JE. Human umbilical cord perivascular cells (HUCPVC): A mesenchymal cell source for dermal wound healing. *Organogenesis* 2010;6:197–203.
  - [27] Yannarelli G, Dayan V, Pacienza N, Lee CJ, Medin J, Keating A. Human umbilical cord perivascular cells exhibit enhanced cardiomyocyte reprogramming and cardiac function after experimental acute myocardial infarction. *Cell Transplant* 2013;22:1651–66.
  - [28] Mordant P, Nakajima D, Kalaf R, Iskender I, Maahs L, Behrens P, et al. Mesenchymal stem cell treatment is associated with decreased perfusate concentration of interleukin-8 during *ex vivo* perfusion of donor lungs after 18-hour preservation. *J Heart Lung Transplant* 2016;35:1245–54.
  - [29] Lalu MM, McIntyre L, Pugliese C, Fergusson D, Winston BW, Marshall JC, et al. Safety of cell therapy with mesenchymal stromal cells (SafeCell): a systematic review and meta-analysis of clinical trials. *PLoS ONE* 2012;7:e47559.
  - [30] Hare JM, Traverse JH, Henry TD, Dib N, Strumpf RK, Schulman SP, et al. A randomized, double-blind, placebo-controlled, dose-escalation study of intravenous adult human mesenchymal stem cells (prochymal) after acute myocardial infarction. *J Am Coll Cardiol* 2009;54:2277–86.
  - [31] Ra JC, Shin IS, Kim SH, Kang SK, Kang BC, Lee HY, et al. Safety of intravenous infusion of human adipose tissue-derived mesenchymal stem cells in animals and humans. *Stem Cells Dev* 2011;20:1297–308.
  - [32] Tolar J, Le Blanc K, Keating A, Blazar BR. Concise review: hitting the right spot with mesenchymal stromal cells. *Stem Cells* 2010;28:1446–55.
  - [33] de Girolamo L, Lucarelli E, Alessandri G, Avanzini MA, Bernardo ME, Biagi E, et al. Mesenchymal stem/stromal cells: a new “cells as drugs” paradigm. Efficacy and critical aspects in cell therapy. *Curr Pharm Des* 2013;19:2459–73.
  - [34] Kurtz A. Mesenchymal stem cell delivery routes and fate. *Int J Stem Cells* 2008;1:1–7.
  - [35] Parekkadan B, Milwid JM. Mesenchymal stem cells as therapeutics. *Annu Rev Biomed Eng* 2010;12:87–117.
  - [36] Elman JS, Murray RC, Wang F, Shen K, Gao S, Conway KE, et al. Pharmacokinetics of natural and engineered secreted factors delivered by mesenchymal stromal cells. *PLoS ONE* 2014;9:e89882.
  - [37] Lee RH, Pulin AA, Seo MJ, Kota DJ, Ylostalo J, Larson BL, et al. Intravenous hMSCs improve myocardial infarction in mice because cells embolized in lung are activated to secrete the anti-inflammatory protein TSG-6. *Cell Stem Cell* 2009;5:54–63.
  - [38] Schrepfer S, Deuse T, Reichenspurner H, Fischbein MP, Robbins RC, Pelletier MP. Stem cell transplantation: the lung barrier. *Transplant Proc* 2007;39:573–6.
  - [39] Gao J, Dennis JE, Muzic RF, Lundberg M, Caplan AI. The dynamic *in vivo* distribution of bone marrow-derived mesenchymal stem cells after infusion. *Cells Tissues Organs* 2001;169:12–20.
  - [40] Eggenhofer E, Benseler V, Kroemer A, Popp FC, Geissler EK, Schlitt HJ, et al. Mesenchymal stem cells are short-lived and do not migrate beyond the lungs after intravenous infusion. *Front Immunol* 2012;3:297.
  - [41] Francois S, Bensidhoum M, Mouseddine M, Mazurier C, Allenet B, Semont A, et al. Local irradiation not only induces

- homing of human mesenchymal stem cells at exposed sites but promotes their widespread engraftment to multiple organs: a study of their quantitative distribution after irradiation damage. *Stem Cells* 2006;24:1020–9.
- [42] Kean TJ, Lin P, Caplan AI, Dennis JE. MSCs: delivery routes and engraftment, cell-targeting strategies, and immune modulation. *Stem Cells Int* 2013;2013:732742.
- [43] Yan C, Li S, Li Z, Peng H, Yuan X, Jiang L, et al. Human umbilical cord mesenchymal stem cells as vehicles of CD20-specific TRAIL fusion protein delivery: a double-target therapy against non-Hodgkin's lymphoma. *Mol Pharm* 2013;10:142–51.
- [44] Mangi AA, Noiseux N, Kong D, He H, Rezvani M, Ingwall JS, et al. Mesenchymal stem cells modified with Akt prevent remodeling and restore performance of infarcted hearts. *Nat Med* 2003;9:1195–201.
- [45] Wang G, Liu LN, Lee K, Buyaner D, Hendricks K, Kalfoglou CS, et al. Comparison of drug and cell-based delivery—engineering adult Mesenchymal cells to deliver human Erythropoietin. *Gene Ther Mol Biol* 2009;13:321–330.
- [46] Chinnadurai R, Garcia MA, Sakurai Y, Lam WA, Kirk AD, Galipeau J, et al. Actin cytoskeletal disruption following cryopreservation alters the biodistribution of human mesenchymal stromal cells *in vivo*. *Stem Cell Reports* 2014;3:60–72.
- [47] Fierro FA, Kalomoiris S, Sondergaard CS, Nolte JA. Effects on proliferation and differentiation of multipotent bone marrow stromal cells engineered to express growth factors for combined cell and gene therapy. *Stem Cells* 2011;29:1727–37.
- [48] Kidd S, Spaeth E, Dembinski JL, Dietrich M, Watson K, Klopp A, et al. Direct evidence of mesenchymal stem cell tropism for tumor and wounding microenvironments using *in vivo* bioluminescent imaging. *Stem Cells* 2009;27:2614–23.
- [49] Vilalta M, Dégano IR, Bagó J, Gould D, Santos M, García-Arranz M, et al. Biodistribution, long-term survival, and safety of human adipose tissue-derived mesenchymal stem cells transplanted in nude mice by high sensitivity non-invasive bioluminescence imaging. *Stem Cells Dev* 2008;17:993–1003.
- [50] Francois S, Usunier B, Douay L, Benderitter M, Chapel A. Long-term quantitative biodistribution and side effects of Human Mesenchymal Stem Cells (hMSCs) engraftment in NOD/SCID mice following irradiation. *Stem Cells Int* 2014;2014:939275.
- [51] Beegle JR, Magner NL, Kalomoiris S, Harding A, Zhou P, Nacey C, et al. Preclinical evaluation of mesenchymal stem cells overexpressing VEGF to treat critical limb ischemia. *Mol Ther Methods Clin Dev* 2016;3:16053.
- [52] Wang P, Zhang Y, Zhao J, Jiang B. Intramuscular injection of bone marrow mesenchymal stem cells with small gap neurotrophin for peripheral nerve repair. *Neurosci Lett* 2015;585:119–25.
- [53] Xie N, Li Z, Adesanya TM, Guo W, Liu Y, Fu M, et al. Transplantation of placenta-derived mesenchymal stem cells enhances angiogenesis after ischemic limb injury in mice. *J Cell Mol Med* 2016;20:29–37.
- [54] Wu SC, Pollak R, Frykberg RG, Zhou W, Karnoub M, Jankovic V, et al. Safety and efficacy of intramuscular human placenta-derived mesenchymal stromal-like cells (cenplacel [PDA-002]) in patients who have a diabetic foot ulcer with peripheral arterial disease. *Int Wound J* 2017;14:823–29.
- [55] Lu D, Chen B, Liang Z, Deng W, Jiang Y, Li S, et al. Comparison of bone marrow mesenchymal stem cells with bone marrow-derived mononuclear cells for treatment of diabetic critical limb ischemia and foot ulcer: a double-blind, randomized, controlled trial. *Diabetes Res Clin Pract* 2011;92:26–36.
- [56] Philippe B, Luc S, Valérie PB, Jérôme R, Alessandra BR, Louis C. Culture and use of mesenchymal stromal cells in phase I and II clinical trials. *Stem Cells Int* 2010;2010:503593.
- [57] Bura A, Planat-Benard V, Bourin P, Silvestre JS, Gross F, Grolleau JL, et al. Phase I trial: the use of autologous cultured adipose-derived stroma/stem cells to treat patients with non-revascularizable critical limb ischemia. *Cytotherapy* 2014;16:245–57.
- [58] Gupta PK, Chullikana A, Parakh R, Desai S, Das A, Gottipamula S, et al. A double blind randomized placebo controlled phase I/II study assessing the safety and efficacy of allogeneic bone marrow derived mesenchymal stem cell in critical limb ischemia. *J Transl Med* 2013;11:143.
- [59] Petrou P, Gothelf Y, Argov Z, Gotkine M, Levy YS, Kassis I, et al. Safety and clinical effects of mesenchymal stem cells secreting neurotrophic factor transplantation in patients with amyotrophic lateral sclerosis: results of phase 1/2 and 2a clinical trials. *JAMA Neurol* 2016;73:337–44.
- [60] Lember N, Idahl LA. Regulatory effects of ATP and luciferin on firefly luciferase activity. *Biochem J* 1995;305(Pt 3):929–33.
- [61] Creane M, Howard L, O'Brien T, Coleman CM. Biodistribution and retention of locally administered human mesenchymal stromal cells: quantitative polymerase chain reaction-based detection of human DNA in murine organs. *Cytotherapy* 2017;19:384–94.
- [62] Glimm H, Oh IH, Eaves CJ. Human hematopoietic stem cells stimulated to proliferate *in vitro* lose engraftment potential during their S/G(2)/M transit and do not reenter G(0). *Blood* 2000;96:4185–93.
- [63] Cashman J, Dykstra B, Clark-Lewis I, Eaves A, Eaves C. Changes in the proliferative activity of human hematopoietic stem cells in NOD/SCID mice and enhancement of their transplantability after *in vivo* treatment with cell cycle inhibitors. *J Exp Med* 2002;196:1141–9.
- [64] Uchida N, He D, Frieria AM, Reitsma M, Sasaki D, Chen B, et al. The unexpected G0/G1 cell cycle status of mobilized hematopoietic stem cells from peripheral blood. *Blood* 1997;89:465–72.
- [65] Maijenburg MW, Noort WA, Kleijer M, Kompier CJ, Weijer K, van Buul JD, et al. Cell cycle and tissue of origin contribute to the migratory behaviour of human fetal and adult mesenchymal stromal cells. *Br J Haematol* 2010;148:428–40.
- [66] Pal R, Hanwate M, Totey SM. Effect of holding time, temperature and different parenteral solutions on viability and functionality of adult bone marrow-derived mesenchymal stem cells before transplantation. *J Tissue Eng Regen Med* 2008;2:436–44.
- [67] Moll G, Alm JJ, Davies LC, von Bahr L, Heldring N, Stenbeck-Funke L, et al. Do cryopreserved mesenchymal stromal cells display impaired immunomodulatory and therapeutic properties? *Stem Cells* 2014;32:2430–42.
- [68] Moll G, Geißler S, Catar R, Ignatowicz L, Hoogduijn MJ, Strunk D, et al. Cryopreserved or fresh mesenchymal stromal cells: only a matter of taste or key to unleash the full clinical potential of MSC therapy? *Adv Exp Med Biol* 2016;951:77–98.
- [69] Mao C, Hou X, Wang B, Chi J, Jiang Y, Zhang C, et al. Intramuscular injection of human umbilical cord-derived mesenchymal stem cells improves cardiac function in dilated cardiomyopathy rats. *Stem Cell Res Ther* 2017;8:18.

## Appendix: Supplementary material

Supplementary data to this article can be found online at doi:10.1016/j.jcyt.2017.09.013.